International Journal of
Advances in Scientific Research and Engineering (ijasre)

E-ISSN : 2454-8006

DOI: 10.31695/IJASRE.2020.33830

Volume 6, Issue 6
June - 2020

Lithostratigraphic Characterization of the Subsurface in Ologbo Community using Wenner-Schlumberger Electrode Configuration of Electrical Resistivity Method

Egbo Okechukwu.[1] and Bright C. Abanum.[2]

[1]Department of Physics, Ambrose Alli University, Ekpoma, Nigeria

[2]Department of Physics, University of Benin, Benin City, Nigeria

ABSTRACT

Wenner-Schlumberger electrode configuration of the electrical resistivity method of geophysical investigation was carried out in Ologbo Community Edo State Nigeria in order to characterize the subsurface geology in this location. The Petrozenith earth resistivity meter was used to measure the resistance offered by the subsurface in two different locations in this geophysical investigation. Sixty (60) Wenner-Schlumberger soundings were carried out in each of the areas. Data were collected and processed using Res2dinv software which produced an inverse model resistivity section which is the true resistivity of the subsurface and this was used to deduce the geological characteristics of the surveyed depth range. Interpretation of the inverse model resistivity section using knowledge of the geology of the study area and standard electrical resistivity of earth materials available in the literature indicates the presence of clayey sand, lateritic clay, laterite, sand and sandstone as the make-up of the subsurface geology of the study area.

Keywords: Wenner-Schlumberger, Geoelectric, lithology, Lateritic clay.

INTRODUCTION

This study was carried out to map out subsurface lithostratigraphic characteristics in the studied location. Subsurface materials such as rocks, minerals and water occur naturally within the earth's surface and establish the raw materials upon which our global society exists and thrives. The geologic makeup of an area is of necessity when considering construction of roads, buildings, and dams for hydropower generation. For example, laterite as a rock type is of immense economic importance. We see the use of laterite as a base course in place of stone in construction of low-density roads. Laterites are widely used to build blocks, build roads, as aquifers in water supply, water treatment etc [1]. Another important economic rock material is the clay mineral. Clay minerals are of great significance among the world's most important and useful industrial mineral. In agriculture, clay minerals are a major component of soil and determinant of soil properties. The clay minerals are important in construction where they are major constituents in bricks and tiles [2]. Even in prehistoric times, sandstone was used for domestic construction and house wares and also used for artistic purposes to create ornamental fountains and statues. In construction, sand is an integral part of concrete, it is used for growing crops, and it is glued to paper to make sandpaper. Previous studies done in this area have been able to show the presence of clay, laterite, sand, and gravel. Therefore, there is a need to investigate a greater depth in search for such valuable materials.

One of the many direct ways in which geophysical investigation aids the general economy is in the delineation of subsurface lithology or rock types which give rise to oil/ mineral, gas and other valuable products of different kinds [3].

Abanum C. Bright worked on determination of groundwater potential using two –dimensional geoelectrical imaging in ologbo of Edo state Nigeria, where he observed that the area is predominantly sand with sparse deposit of clay and hence the studied area may hold good prospect for groundwater in view of the probable thick aquifer layer [4].

The geoelectric method of geophysical investigation utilizes the electrical properties of the subsurface materials to differentiate the subsurface into geoelectric layers and sections. Geoelectric resistivity is one of the variables which are the physical properties of the rock layer below the subsurface. Rock resistivity data can be used to develop a model of subsurface and stratigraphic structures in terms of electrical properties. Geoelectric resistivity depends on lithology, air content, porosity and pore ion concentration [5].

2. LOCAL GEOLOGIC SETTINGS

Ologbo community is located in Ikpoba-Okha Local government area of Edo State. The community is essentially rural and its geographical coordinates are 6°3′0″North and 5°40′0″ East. The geology of this research area is characterized by deposits laid during tertiary and cretaceous periods. The area is underlain by sedimentary rock constituting part of the Benin Formation which is made up of over 90% massive, porous, coarse sand with clay/shale inter-beds having high groundwater retention capacity [6]. Soil particles vary from coarse grained to fine grained in some areas, poorly sorted, sub-angular to well-rounded particles with ignite streaks and fragment.

Ologbo Formation is aquiferous in nature due to its very low percentage of shaly layers having a depth of about 2445m with no overpressure [7]. This community falls within the well-known rainforest belt of Nigeria, with dual seasons; wet season (March to October) and the dry season period (November to March) the following year.

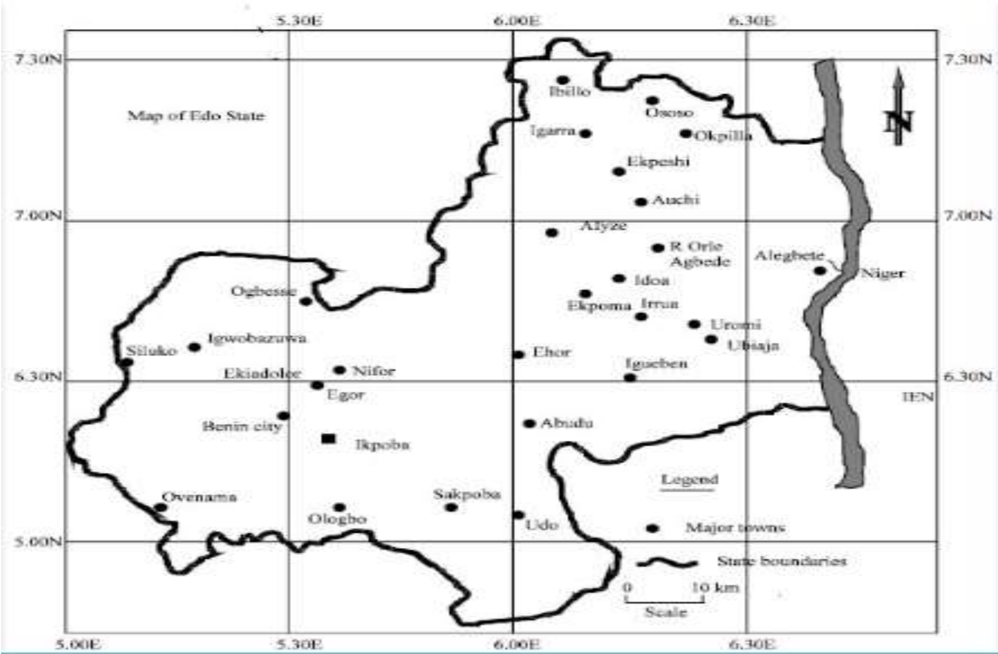

***Figure 1*: Map of Edo State Showing Ologbo [8].**

2.1 Theory

The geoelectrical method of geophysical investigation is capable of locating both low and high resistive formations, therefore it is an important tool for characterizing subsurface lithology [9]. Due to the inhomogeneity of soils, the resistivity of soils varies with depth. Soil resistivity is a complicated function of permeability, ionic content of the pores fluids, clay mineralization and porosity [10].

Geoelectrical investigation is carried out by measuring the electrical potential (V) resulting from current input (I) into the ground with the purpose of achieving information on the resistivity structure in the ground. The resistance is obtained using Ohm's law

$$R = \frac{V}{I} \qquad 1$$

And then the apparent resistivity is computed using the equation,

$$\rho_a = KR \qquad 2$$

Where K is the geometric factor which depends on the arrangement of the four electrodes [11]. The electrical resistivity method involves the measurement of the apparent resistivity of soils and rock as a function of depth. It is expressed in ohm-meters [12].

DOI: 10.31695/IJASRE.2020.33830

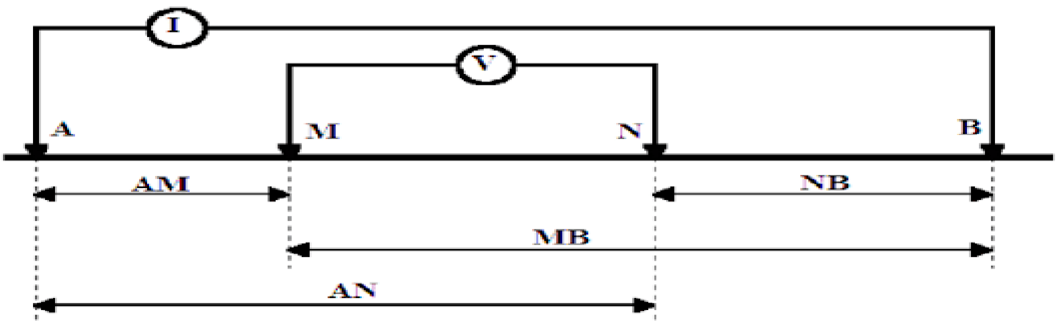

***Figure 2*: Generalized electrode configuration for resistivity measurement.**

Consider a single point electrode, located on the boundary of a semi-infinite, electrically homogenous medium, which represents a fictitious homogenous earth. If the electrode carries a current I, measured in amperes (A), the potential difference (V) across a hemispherical shell of incremental thickness δr is given by:

$$\frac{V}{\delta r} = -\rho . j \qquad 3$$

The current density (j) is the current (I) divided by the area over which the current is distributed (for a hemisphere, the area is $2\pi r^2$) so that the above equation becomes

$$\frac{V}{\delta r} = -\rho \frac{I}{2\pi r^2} \qquad 4$$

Thus the voltage V_r at a point r from the current point source is:

$$V_r = \int V = -\int \rho . \frac{I\delta r}{2\pi r^2} = \frac{\rho I}{2\pi} . \frac{1}{r} \qquad 5$$

For a current source and sink, the potential V_P at any point P in the ground is equal to the sum of the voltage from the two electrodes, such that: $V_P = V_A + V_B$ where V_A and V_B are the potential contributions from the two electrodes, A(+I) and B(−I). The potentials at electrode M and N are:

$$V_M = \frac{\rho I}{2\pi}\left[\frac{1}{AM} - \frac{1}{MB}\right] \qquad 6$$

$$V_N = \frac{\rho I}{2\pi}\left[\frac{1}{AN} - \frac{1}{NB}\right] \qquad 7$$

The potential difference (δV) is given by;

$$\delta V_{MN} = V_M - V_N \qquad 8$$

$$\delta V_{MN} = \frac{\rho I}{2\pi}\left\{\left[\frac{1}{AM} - \frac{1}{MB}\right] - \left[\frac{1}{AN} - \frac{1}{NB}\right]\right\} \qquad 9$$

Solving and making the resistivity ρ the subject we have

$$\rho = 2\pi \frac{\delta V_{MN}}{I}\left\{\left[\frac{1}{AM} - \frac{1}{MB}\right] - \left[\frac{1}{AN} - \frac{1}{NB}\right]\right\}^{-1} \qquad 10$$

$$\boldsymbol{K} = 2\pi \left\{\left[\frac{1}{AM} - \frac{1}{MB}\right] - \left[\frac{1}{AN} - \frac{1}{NB}\right]\right\}^{-1} \qquad 11$$

Which is the geometric factor depending on the arrangement of the four electrodes.

For Wenner-Schlumber configuration, AM= na , $= na + a$, $AN = na + a$, and $NB = na$

Substituting these into eqn. (11) we have

DOI: 10.31695/IJASRE.2020.33830

$$\boldsymbol{K} = 2\pi \left\{ \left[\frac{1}{na} - \frac{1}{na+a} \right] - \left[\frac{1}{na+a} - \frac{1}{na} \right] \right\}^{-1}$$

$$\boldsymbol{K} = 2\pi \left\{ \left[\frac{na+a-na}{na(na+a)} \right] - \left[\frac{na-(na+a)}{na(na+a)} \right] \right\}^{-1}$$

$$\boldsymbol{K} = 2\pi \left\{ \left[\frac{a}{na(na+a)} \right] - \left[\frac{-a}{na(na+a)} \right] \right\}^{-1}$$

$$\boldsymbol{K} = 2\pi \left\{ \left[\frac{2}{na(n+1)} \right] \right\}^{-1}$$

$K = 2\pi \left(\frac{na(n+1)}{2} \right) = \pi na(n+1)$ 12

From Ohm's law, $\boldsymbol{R} = \frac{\delta V_{MN}}{I}$, equation (8) reduces to

$\boldsymbol{\rho} = \boldsymbol{KR}$ 13

Where **K** is the geometric factor which depends on the arrangement of the four electrodes.

Where the ground is not uniform, the resistivity so calculated is called the apparent resistivity (ρa) because these measurements are made over a real heterogeneous earth, as distinguished from the fictitious homogenous half-space, the symbol $\boldsymbol{\rho}$ is replaced by $\boldsymbol{\rho_a}$ for apparent resistivity.

$\rho_a = KR$ 14

Methods

For this research work, data was acquired using Petrozenith earth resistivity meter.

Figure 1: Petrozenith Earth Resistivity Meter Setup.

The electrical resistivity technique employed is the Wenner-Schlumberger hybrid configuration. Wenner-Schlumberger technique is a configuration with a constant system of spacing rules with a note of factor "n" as this configuration is the comparison of the distance between C1-P1 (or C2-P2) electrodes with spaces between P1-P2 as in figure 2. If the distance between electrodes. The potentials (P1 and P2) are 'a' than the distance between the current electrode (C1 and C2) is 2na + a [13].

DOI: 10.31695/IJASRE.2020.33830

This procedure utilizes 4 electrodes placed in a straight line and combines both the Wenner and Schlumberger configuration for determining the resistance offered by the subsurface. For the particular measurement for which the spacing factor 'n'is equal to 1, this technique takes the form of measurement in the Wenner configuration but for measurements for n = 2, 3, 4 and so on, then Wenner-Schlumberger technique is the same as the Schlumberger configuration. The current electrode and the potential electrode are greater than the distance between the potential electrodes.

Using this technique, data were acquired and the resistivity imaging were interpreted geologically using the standard resistivity values for rocks, minerals and sediments from available literatures and also using the knowledge of the local geology of the research area. Table 1 shows some earth materials and their respective resistivity.

Table 1: Electrical Resistivity of Some Earth Material [14].

ROCK MATERIAL	RESISTIVITY (Ohm-meter)
Top soil	50 - 1,000
Alluvium	25 – 1,500
Syenite	100 - 100,000
Gnesis	200 – 34,000
Granite	300 – 20,000
Basalt	200 – 20,000
Marble	100 – 200,000
Quartzite	10 – 200,000
Gabbio	15,000
Schist	50 – 10,000
Biorite	50,000
Shale	80 – 20,000
Sandstone	30 – 500,000
Clay-shale	0.00004 – 900
Limestone	30 – 500,000
Clay	1 – 100
Fresh Groundwater	10 – 100
Loams	10 – 450
Sand	100 – 500,000
Marl	50 – 90
Oil Sands	60 – 900

3. RESULTS AND DISCUSSION

Geoelectrical investigation of the subsurface was carried out. The resistance offered by the subsurface materials was measured by the Petrozenith earth resistivity meter by appropriately measuring the electrical potential (V) resulting from the current input (I) into the ground and from Ohm's law $R = \frac{V}{I}$ the resistance values was recorded. The apparent resistivity ρ_a was computed using the equation, $\rho_a = KR$

Two locations were investigated in the study area each of 200 m in length and data were collected. Res2dinv software was used to process the data. Geoelectric imaging consisting of three figures was obtained. The upper modeled with the raw apparent resistivity. The middle represents model of the computer generated apparent resistivity data. These two figures are termed pseudosection. The lower figure is produced with the inverted apparent resistivity data, which is the true subsurface resistivity. This lower figure is what is used to deduce the geological characteristics of the surveyed depth range. The result obtained from each of these survey lines are presented in Tables 2 and 3.

DOI: 10.31695/IJASRE.2020.33830

TRAVERSE 3: BEGIN, LAT. 06˚04'27.5" LONG. 05˚39'18.6" Elev. 18.4m
END, LAT. 06˚04'27.4" LONG. 05˚39'12.2" Elev. 21.7m
LOCATION : OZOLUA GRAMMAR SCHOOL , OLOGBO, EDO STATE
SURVEY DATE: 24/10/2018

Table 2: Resistivity Data for Traverse 3

Electrode Location a = 10, n = 1, k = 62.84					
C1	P1	P2	C2	R (Ω)	ρ (Ωm)
0	10	20	30	2.7	1866
10	20	30	40	11.27	2432
20	30	40	50	8.65	2294
30	40	50	60	9.62	1546
40	50	60	70	7.71	2551
50	60	70	80	10.45	727
60	70	80	90	2.32	2105
70	80	90	100	14.64	1734
80	90	100	110	12.51	1678
90	100	110	120	11.27	281
100	110	120	130	10.98	302
110	120	130	140	9.7	311
120	130	140	150	7.35	357
130	140	150	160	7.73	310
140	150	160	170	6.31	383
150	160	170	180	6.22	451
160	170	180	190	24.8	364
170	180	190	200	24.2	1571
Electrode Location a = 10, n = 2, k = 125.68					
0	20	40	60	0.422	1847
10	30	50	70	15.33	1443

DOI: 10.31695/IJASRE.2020.33830

20	40	60	80	15.65	1714
30	50	70	90	15.44	2174
40	60	80	100	15.56	1673
50	70	90	110	17.78	1359
60	80	100	120	17.91	1565
70	90	110	130	15.82	1381
80	100	120	140	16.04	1279
90	110	130	150	17.27	1340
100	120	140	160	15.49	1262
110	130	150	170	12.49	1235
120	140	160	180	13.52	1284
130	150	170	190	12.66	1150
140	160	180	200	11.28	1278
Electrode Location a = 10, n = 3, k = 188.52					
0	30	60	90	2.02	1182
10	40	70	100	8.47	1382
20	50	80	110	8.83	1621
30	60	90	120	11.5	1484
40	70	100	130	9.71	1354
50	80	110	140	9.16	1193
60	90	120	150	9.15	1278
70	100	130	160	8.69	1037
80	110	140	170	8.35	1248
90	120	150	180	6.95	1171
100	130	160	190	6.97	1129
110	140	170	200	7.42	1037
Electrode Location a = 10, n = 4, k =251.36					
0	40	80	120	3.73	993
10	50	90	130	5.74	1430
20	60	100	140	6.24	1493
30	70	110	150	6.5	1312
40	80	120	160	6.14	1264
50	90	130	170	6.01	1217
60	100	140	180	5.72	1259
70	110	150	190	5.64	1051
80	120	160	200	5.48	1108
Electrode Location a = 10, n = 5, k = 314.2					
0	50	100	150	0.121	1078
10	60	110	160	3.89	1332
20	70	120	170	4.59	1379
30	80	130	180	4.85	1329
40	90	140	190	4.23	1244
50	100	150	200	4.5	1093

DOI: 10.31695/IJASRE.2020.33830

TRAVERSE 8: BEGIN, LAT. 06˚04'49.6" LONG. 05˚39'41.9" Elev. 22.4m

END, LAT. 06˚04' `56.1" LONG. 05˚39' 41.8" Elev. 28.2m

LOCATION: Imasabor Road, Ologbo, Edo State.

SURVEY DATE: 26/10/2018

Table 3: Resistivity Data fo

Electrode Location a = 10, n = 1, k = 62.84					
C1	P1	P2	C2	R (Ω)	ρ (Ωm)
0	10	20	30	2.7	635
10	20	30	40	11.27	585
20	30	40	50	8.65	498
30	40	50	60	9.62	452
40	50	60	70	7.71	476
50	60	70	80	10.45	586
60	70	80	90	2.32	524
70	80	90	100	14.64	588
80	90	100	110	12.51	796
90	100	110	120	11.27	882
100	110	120	130	10.98	1042
110	120	130	140	9.7	1208
120	130	140	150	7.35	1022
130	140	150	160	7.73	1019
140	150	160	170	6.31	1021
150	160	170	180	6.22	876
160	170	180	190	24.8	887
170	180	190	200	24.2	803
Electrode Location a = 10, n = 2, k = 125.68					
0	20	40	60	0.422	1065
10	30	50	70	15.33	743
20	40	60	80	15.65	613
30	50	70	90	15.44	682
40	60	80	100	15.56	659
50	70	90	110	17.78	720
60	80	100	120	17.91	900
70	90	110	130	15.82	1075
80	100	120	140	16.04	1027
90	110	130	150	17.27	1208
100	120	140	160	15.49	1230
110	130	150	170	12.49	1117
120	140	160	180	13.52	1127
130	150	170	190	12.66	1115
140	160	180	200	11.28	1061
Electrode Location a = 10, n = 3, k = 188.52					
0	30	60	90	2.02	649
10	40	70	100	8.47	818

DOI: 10.31695/IJASRE.2020.33830

20	50	80	110	8.83	892
30	60	90	120	11.5	956
40	70	100	130	9.71	924
50	80	110	140	9.16	1039
60	90	120	150	9.15	1101
70	100	130	160	8.69	1393
80	110	140	170	8.35	1231
90	120	150	180	6.95	1097
100	130	160	190	6.97	1114
110	140	170	200	7.42	1214
Electrode Location a = 10, n = 4, k =251.36					
0	40	80	120	3.73	980
10	50	90	130	5.74	1481
20	60	100	140	6.24	1217
30	70	110	150	6.5	1239
40	80	120	160	6.14	1156
50	90	130	170	6.01	1322
60	100	140	180	5.72	1403
70	110	150	190	5.64	1428
80	120	160	200	5.48	1224
Electrode Location a = 10, n = 5, k = 314.2					
0	50	100	150	0.121	1043
10	60	110	160	3.89	2196
20	70	120	170	4.59	1618
30	80	130	180	4.85	1351
40	90	140	190	4.23	1323
50	100	150	200	4.5	1213

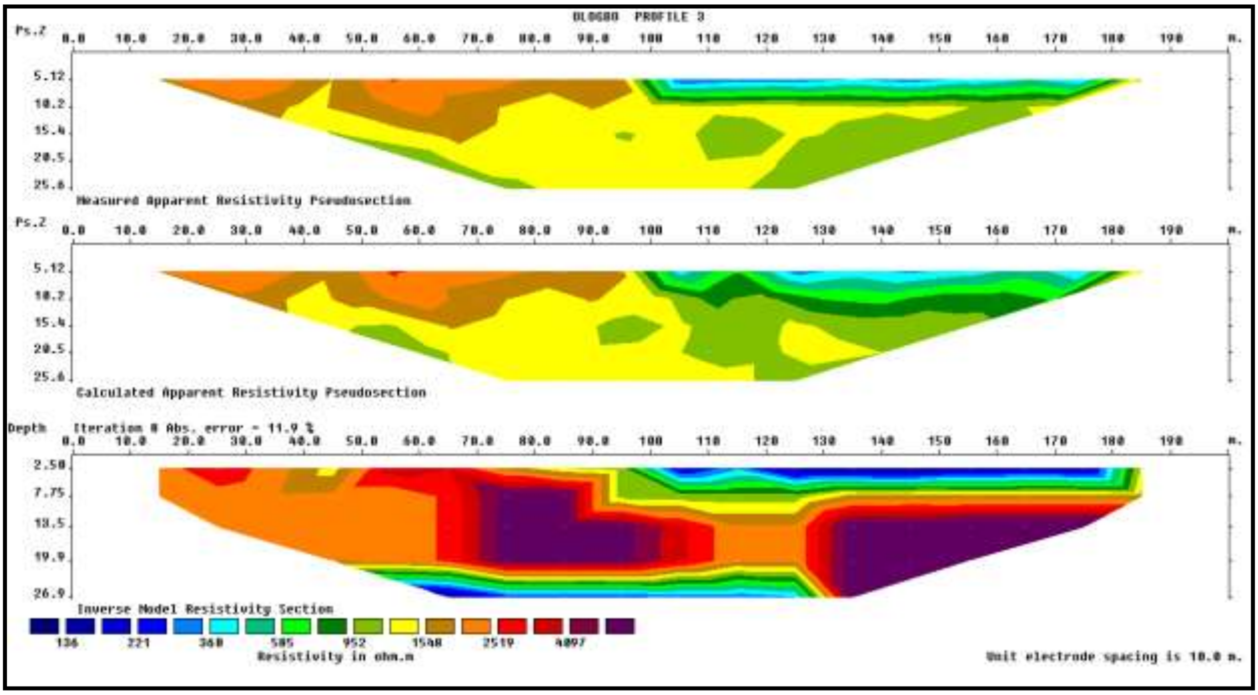

Figure 3: **Resistivity Imaging Of Profile 3**

DOI: 10.31695/IJASRE.2020.33830

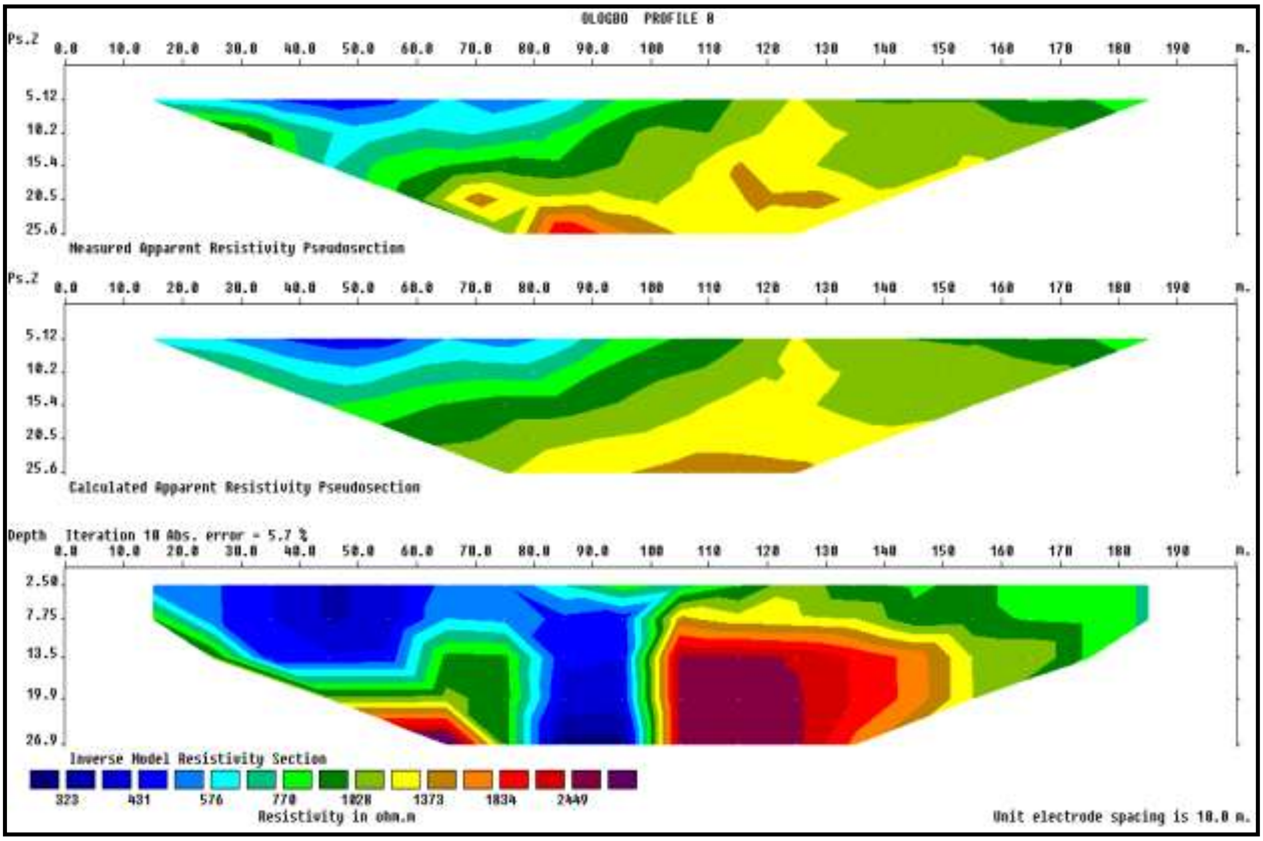

Figure 4: Resistivity Imaging Of Profile 8

4. INTERPRETATION

The resistivity imaging representing the variation of resistivity with depth along profile 3 is shown in figure 3. The low resistive material with apparent resistivity values 136 – 360 Ωm is interpreted to be clayey-sand Formation. This Formation spreads laterally from 105 m – 180 m along the profile with a depth of about 3 m. Underlain by this clayey-sand Formation are layers with apparent resistivity between 360 – 1548 Ωm which depicts a lateritic soil Formation. Sections with apparent resistivity values between 1548 – 2519 Ωm is interpreted to be lateritic sand Formation which occurs between 15 m – 63 m and 110 m – 128 m along the profile with depth penetration of about 20 m. Enclosed is a high resistive zone of apparent resistivity of above 4097 Ωm which is interpreted to be sandstone and occurs at a depth of about 5 m – 19.9 m with lateral extent from 70 m – 100 m along the profile. This high resistive zone is also seen along the profile from 130 m beyond the extent of investigation and at depth of about 11 m beyond the depth of investigation.

The resistivity imaging for profile 8 which shows the variation of resistivity along the profile with depth is shown in figure 4 above. Along the profile, there is a section of low resistive material which ranges from 323 Ωm to 576 Ωm suggestive of lateritic clay. This section has a lateral extension from 15 m to 70 m along the profile with a depth of about 14.5 m which consists of four moderately consistent layers. This low resistivity section is also seen from 80 m to 100 m along the profile which extends downward beyond the depth of investigation. Below this laterite clay is underlain by layers with apparent resistivity value of range 576 Ωm to 1028 Ωm spreading from 15 m to 80m and also seen between 98 m to 180 m along the profile which indicates the presence of lateritic material Underlain this are four layers with apparent resistivity values ranging from 1028 Ωm – 1373 Ωm interpreted to be lateritic sand. Layers with resistivity values with range from 1373 Ωm – 1834 Ωm is interpreted to be wet sand. Layers with resistivity values which ranges from 1834 Ωm – 2449 Ωm and above is interpreted to be dry sand. The last layer which is composed of a high resistive zone with apparent resistivity value of 2449 Ωm and above indicates the presence of sandstone. This appears like a dome-like structure which extends beyond the depth of investigation.

DOI: 10.31695/IJASRE.2020.33830

5. CONCLUSION

This study was carried out using Wenner – Schlumberger configuration of electrical resistivity method to characterize the lithostratigraphy of the subsurface in the study location. Res2dinv software was used to process the data from each of the surveyed profile. Geoelectric imaging consisting of three figures were obtained and are interpreted to generate the subsurface geologic characteristics.

The analysis and interpretation of the results shows the presence of clayey sand, lateritic clay, laterite, sand and sandstone as the make-up of the subsurface of the study area. The litghostratigrafic units are predominantly sandy and lateritic.

REFERENCES

1. Adekunle, A., Ekandem, E. S., Ibe, k., Ananso, G.N., Mondigha, E.B., (2014). Analysis of thermal and electrical properties of laterite, clay and sand samples and their effect on inhabited buildings in Ota, Ogun State, Nigeria. Journal of Sustainable Development Studies, ISSN 22014268, Volume 6, Number 2, 391-412.
2. Suzanne Christine Aboudi Mana, Marlia Mohd Hanafiah and Ahmed Jala Khan Chowdhury (2017) Environmental characteristics of clay and clay-based minerals, Geology, Ecology, and Landscapes, 1;3, 155-161, DOI: 10.1080/24749508.2017.1361128
3. Ezomo, F.O and Ifedili, S.O., (2005). Determination of water bearing formations at Osasogie Quarters by electrical Resistivity method. Journal of civil and Environ. Systems Engr. 6(1), 1-12.
4. Abanum C. Bright.; Two-dimensional electrical imaging techniques for determination of groundwater potential in edo state, Nigeria, International journal of modern applied physics, 10(1), (2020): 1-15
5. A. Mangeney, et al, A numerical study of anisotropic, low Reynolds number, free surface flow for ice sheet modeling, (Journal of Geophysical Research: Solid Earth, 1997), pp. 22749-22764
6. Akpokodje, E.U, & Etu-Efeotor, J.O (1987). The occurrence and economic potential of clean sand deposits of the Niger Delta. Journal of African Earth Sciences, Vol. 6 (1), pp. 61 – 65.
7. Aisabokhae J.E., Adagbon J.E (2016). Geophysical Determination of Construction Clay Deposit Using 2-Dimensional Resistivity Imaging In Ologbo Area of Edo State. Research & Reviews: Journal of Physics. 5(2): 1-12p.
8. Ozegin, K.O., Ataman, O.J. and Jegede, S.I. (2017). Dumpsite Characterization in Ekpoma from Integrated Surface Geophysical Methods. Physical Science International Journal. 15 (4). 1-11.
9. Sørensen K.I, Auken E, Christensen NB, Pellerin L 2005 J. Society of Exploration Geophysics 13 585–603.
10. Kizlo, M., and Kanbergs, A. (2009). The Causes of the Parameters Changes of Soil Resistivity. The 50th International Scientific Conference, Power and Electrical Engineering, 43-46.
11. Agogo, G.E: The electrical resistivity log as an aid in determining some reservoir characteristics. Petroleum Trans. A.I.M.E. 2009; 46:54-62.
12. Ezomo, F.O., Justice .E. Adagbon, Ojeabu Akhirevbulu, and Ezekiel Abriku (2015). Delineation of Subsurface Lithology using Two- Dimensional Geoelectrical Resistivity Imaging in Ologbo Area of Edo State, Nigeria. International Journal of Scientific and Engineering Research, 6(6):1110-1118.
13. Jamaluddin and Emi Prasetyawati Umar (2018). Identification of Subsurface Layer with Wenner-Schlumberger Arrays Configuration Geoelectrical Method. Global Colloquium on GeoSciences and Engineering. IOP Conf. Ser.: Earth Environ. Sci. 118 012006.
14. Reynolds, J.M. (1997). An Introduction to Applied and Environmental Geophysics. John Willey and Sons Ltd., Chichester, UK, pp497.

DOI: 10.31695/IJASRE.2020.33830